Metabasin transitions are Johari-Goldstein relaxation events

Marcus T. Cicerone, and Madhusudan Tyagi

Citation: The Journal of Chemical Physics **146**, 054502 (2017);
View online: https://doi.org/10.1063/1.4973935
View Table of Contents: http://aip.scitation.org/toc/jcp/146/5
Published by the American Institute of Physics

Metabasin transitions are Johari-Goldstein relaxation events

Marcus T. Cicerone[1,2,a] and Madhusudan Tyagi[1,3]
[1]*National Institute of Standards and Technology, Gaithersburg, Maryland 20899-8543, USA*
[2]*Institute for Physical Sciences and Technology, University of Maryland, College Park, Maryland 20742-2431, USA*
[3]*Department of Materials Science and Engineering, University of Maryland, College Park, Maryland 20742, USA*

(Received 21 October 2016; accepted 29 December 2016; published online 1 February 2017)

We show that by representing quasi-elastic and inelastic neutron scattering from propylene carbonate (PC) with an explicitly heterogeneous model, we recover signatures of two distinct localized modes in addition to diffusive motion. The intermediate scattering function provides access to the time-dependence of these two localized dynamic processes, and they appear to correspond to transitions between inherent states and between metabasins on a potential energy landscape. By fitting the full q-dependence of inelastic scattering, we confirm that the Johari-Goldstein (β_{JG}) relaxation in PC is indistinguishable from metabasin transitions. [http://dx.doi.org/10.1063/1.4973935]

I. INTRODUCTION

It has become clear over the past several decades that dynamic heterogeneity (DH) underlies the characteristic behavior of transport and relaxation processes in glasses and supercooled liquids. The first experimental confirmations of this for glass-forming systems at low temperatures came in the 1990s and were focused on time scales of milliseconds and longer.[1–4] However, experimental methods have not been particularly effective at extracting real-space dynamics on a molecular lengthscale, and only a few general properties of long-time DH have been established, such as approximate lengthscale[5–8] and lifetime.[3,4,9] By contrast, DH at much shorter times, discovered in the 1980s,[10,11] was accessible to simulation and could be characterized in much greater detail.

Simulation studies show that DH at the shortest times appears in the form of intermittent localized molecular rearrangements. Building on the potential energy landscape (PEL) concept,[12] Stillinger described these discrete rearrangement events[10] in terms of barrier crossings on a high-dimensional PEL with shallow minima corresponding inherent structures (ISs), which decorate deeper minima, referred to as metabasins (MBs).[13] It is suggested that transitions between ISs within a MB are associated with local cage distortions, while transitions between MBs involve collective rearrangements of a small number of particles.[14] MB transitions are spatially heterogeneous relaxation events[15] and thus appear to be the fundamental element of short-time DH.

Connections have been established between these microscopic collective motions involving particle rearrangements and macroscopic relaxation processes, including self-diffusion[16–20] and α relaxation.[17] A connection to the Johari-Goldstein[21] (β_{JG}) relaxation process has also become increasingly appreciated. However, the precise nature of this relaxation process remains an outstanding question.

Stillinger suggested that β_{JG} relaxations correspond to IS transitions in the PEL, with sequential β_{JG} relaxations leading to MB transitions and α relaxation.[22] However, Vogel *et al.* have alternatively proposed that the exploration of the MB (i.e., a series of IS transitions) should be associated with β_{JG} relaxation.[15] By contrast, we note that there are many remarkable similarities between β_{JG} relaxation and transitions between MBs, suggesting that they may be one and the same. Some of these similarities are as follows: (i) The β_{JG} process appears to bifurcate from the α relaxation when relaxation times are approximately 1 ns, and just when thermal energies are comparable to the heights of potential barriers on the PEL,[12] and when ergodicity times begin to increase substantially.[23] Incidentally, this is the same point at which one expects that the localized molecular reorganization events will become discrete and intermittent rather than occurring continuously.[24] (ii) Rapid rotational jumps of (6°–10°) are found for β_{JG} relaxation above T_g.[25,26] Assuming that the Stokes-Einstein relation holds locally, this corresponds to spatial excursions of $0.2\,r_H$ (where r_H is the hydrodynamic radius), and Vogel *et al.*[15] found spatial excursions $0.2\,r_H$ to be the characteristic of MB transitions. (iii) The dielectric β_{JG} loss peak exhibits a thermal hysteresis that can be modeled as a relaxation between basins in an asymmetric double well potential,[27] similar to the localized transitions between local minima in the PEL. (iv) It is clear that excursions associated with β_{JG} relaxation must occur as a rapid series of smaller steps[28] and are collective in nature.[21] This is consistent with collective, multi-step rearrangement[11] characteristic of MB transitions. (v) The temperature dependencies of the peak time ($t^\star$) in the non-Gaussian parameter, characterizing short time DH,[17] the mean waiting time between MB transitions,[16] and the temperature dependence of the β_{JG} relaxation time ($\tau_{\beta,JG}$)[29] all follow the diffusion coefficient (D_T), at least to temperatures as low as the mode-coupling critical temperature T_c.[16]

Neutron scattering is an ideal tool for investigating the detailed motion of liquids on the time scales and lengthscales germane to the β_{JG} relaxation. In fact, we show below that

[a]cicerone@nist.gov

direct signatures of IS transitions, MB transitions, and β_{JG} relaxation are present in the neutron scattering. From these signatures, we show quite clearly that β_{JG} relaxation is to be identified with MB transitions. Although neutron scattering has been applied to liquids and glasses for decades, these signatures have not been identified until now. This is probably because, exceptions notwithstanding,[19,30,31] neutron scattering from molecular liquids has historically been analyzed in terms of homogeneous models[32,33] in spite of overwhelming evidence for short-time DH in these systems.

II. THE MODEL

In this work, we use an explicitly heterogeneous dynamics model to describe the scattering function $S(q,E)$. We account for distinct types of motion expected in amorphous systems: over-damped vibration (in which we include IS transitions), motion associated with MB transitions, and homogeneous diffusive motion. Based on ultrafast optical experiments performed by us and on recent work by Vispa *et al.*,[31] we choose Lorentzians to represent each of the three types of motion considered here. Vispa *et al.*,[31] recently found that a triple Lorentzian function provided significantly better fits for $S(q,E)$ of a molecular liquid than common models of similar complexity containing functional forms such as KWW and Gaussian, and much better fits than 2-component models. In accordance with Vispa's finding, we observe three exponential relaxation processes for propylene carbonate (PC) in time-domain optical Kerr effect data covering similar time and lengthscales to those considered here (manuscript in preparation). Accordingly, we propose the following model for $S(q,E)$:

$$\begin{aligned} S(q,E) = {} & (1-\tilde{\Phi}(E))L_D \otimes [(1-a_v)\,\delta(E) + a_v L_v] \\ & + \tilde{\Phi}(E)L_D \otimes [(1-a_v)\,\delta(E) + a_v L_v] \\ & \otimes [(1-a_h)\,\delta(E) + a_h L_h], \end{aligned} \tag{1}$$

where $L_i = \Gamma_i \pi^{-1}(E^2 + \Gamma_i^2)^{-1}$, $\otimes$ is the convolution operator, the convolutions are over frequency (energy). $\Gamma_D = D_T q^2$, where D_T is the diffusion coefficient, and a_v and a_h are, respectively, q-dependent scattering amplitudes from vibration and hopping. Anticipating that these two will be localized modes with Gaussian distributions of displacements,[32] we assume the functional form

$$a_i(q) = c_i\{1 - \exp[-(\pi\sigma_i q)^2]\}, \tag{2}$$

where σ_i represents the characteristic lengthscales of motion for mode i.

The two terms in Eq. (1) account for two dynamically different classes of molecules. We assume that all molecules undergo both diffusion and over-damped vibrations at all times. Accordingly, both terms in Eq. (1) include diffusive (D) and vibrational (v) motion. We also assume that, at a given instant, only some fraction[15] (Φ) of molecules can also execute collective hopping motion (h) associated with MB transitions. These are accounted for in the second term of Eq. (1).

The meaning of Φ is of particular interest. In order to explain it more clearly, we first give the time-domain representation of Eq. (1) as

$$\begin{aligned} F(q,t) = {} & e^{-t/\tau_D}[1 + a_v(e^{-t/\tau_v} - 1)] \\ & \times [(1-\Phi(t)) + \Phi(t)(1 + a_h(e^{-t/\tau_h} - 1))], \end{aligned} \tag{3}$$

where $\tau_i = \hbar/\Gamma_i$. As an aside, we note that, in the regime $t\Gamma_D \ll \hbar \ll t\Gamma_h \leq t\Gamma_v$, we can ignore terms involving τ_v and τ_h, and Eq. (3) reduces essentially to

$$F(q) = (1-\Phi(t))e^{-(q\pi\sigma_v)^2} + \Phi(t)e^{-(q\pi\sigma_h)^2}, \tag{4}$$

which we had previously used to fit quasielastic neutron scattering (QENS) on several liquids, including PC.[19] Both equations yield similar values for fit parameters, but we use the full model here.

From Eq. (3), we see that the parameter $\Phi(t)$ represents the fraction of molecules that have hopped (undergone a MB transition) up to time t. Bearing in mind that hops constitute significantly larger excursions than vibrations, it is clear that until a molecule executes a hop, the q-dependence of its scattering signature will be characteristic of only small lengthscale motion. Once a hop occurs, that signature will change to larger lengthscale for all subsequent times.

We can describe the nature of $\Phi(t)$ more clearly through appeal to a minimal model with two dynamic states. Within this model, molecules can undergo collective rearrangements (MB transitions) in one state and not in the other. Given the emerging connection between local structure and dynamics,[34,35] we assume an association between local ordering and ability to execute collective motion that is not critical to, but is convenient for our purposes here. We envision that molecules which are locally more highly ordered or tightly caged (TC) have barriers between MBs that are too high to overcome. Likewise, we imagine that molecules in slightly less ordered regions are more loosely caged (LC) and have smaller barriers between MBs allowing these transitions to occur more easily. We can reasonably equate LC regions with local excitations envisioned by Garrahan and Chandler[36] and which are central to facilitation ideas.

We assume a dynamic equilibrium between TC and LC states, $TC \rightleftharpoons LC$ with forward (k_{TL}) and backward (k_{LT}) rates, for which we define

$$\Phi_0 \equiv \frac{n_{LC}}{n_{LC} + n_{TC}}, \tag{5}$$

where the n_{LC} and Φ_0 are, respectively, the instantaneous number and fraction of molecules undergoing MB transitions in LC domains. We detect TC or LC states only through the statistical properties of their displacements, which develop as molecules explore the cage formed by their neighbors, and this occurs on a time scale of ≈1 ps.[20,37] Accordingly, we set $\Phi_0 = \Phi(1\text{ ps})$, and an expression for $\Phi(t)$, valid for t > 1 ps, can be written as

$$\Phi(t) = \Phi_0 + \int_0^t (1-\Phi(t'))\,k_{TL}(t')dt', \tag{6}$$

where $\Phi(t) = \Phi_0 + (1 - e^{-t/\tau_{TL}})$ if k_{TL} is constant in time. We note that τ_{TL} is the same as the persistence time, τ_p in facilitation

theories.[38] We can view the quantity $(1 - \Phi(t))$ as a relaxation function since it gives the fraction of molecules that have, up to time t, not yet participated in an MB transition.

Above we have described the physical meaning of all the model parameters except τ_v and τ_h. Through the examination of experimental data, we will see that these appear to represent the characteristic times for IS transitions and MB barrier crossing events, respectively. We will also see through the time dependence of the σ_i parameters that we obtain a MB exploration time, τ_{MX}.

In what follows, we confirm the validity of our model and explore its implications using quasielastic neutron scattering (QENS) and incoherent inelastic neutron scatteirng (INS) from propylene carbonate (PC). We chose PC for this study because it lacks strongly directional intermolecular interactions, and its only intramolecular motion, a methyl rotor, exhibits dynamics outside the lengthscale and time scale of interest,[39] as discussed in the supplementary material.

III. RESULTS

A. Quasielastic neutron scattering—Experimental

QENS data were collected using the Disk Chopper Spectrometer (DCS)[40] at the NIST neutron center on NG4 with neutron wavelength $\lambda \approx 4.0$ Å, q in the range (0.22–2.77) Å^{-1}, and energy resolution of 200 μeV. Background was accounted for (see the supplementary material for more details).

Figure 1 shows the fit of Eq. (1) to quasielastic neutron scattering (QENS) from PC at 300 K and q = 0.8 Å^{-1}. The model is convolved with the instrument resolution, which is estimated as a Gaussian from sample scattering at 30 K. We used an iterative simulated annealing algorithm to find optimized fit parameters, a_i and Γ_i at each average q value. The upper trace shows fit residuals (H-D), normalized by the standard deviation (sd) at each data point. These normalized residuals are randomly distributed between −1 and 1 for all data reported, as exemplified in Fig. 1.

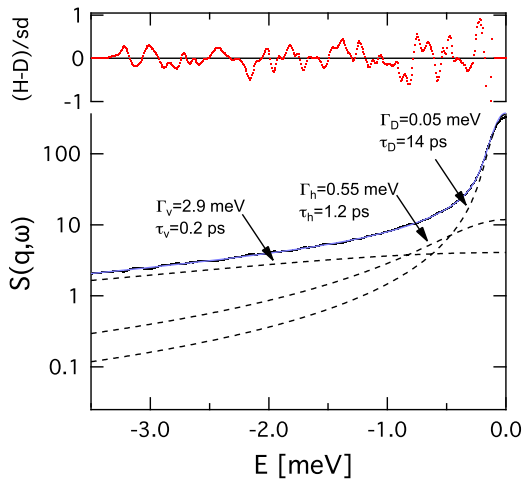

FIG. 1. Fits to $S(q = 0.8$ Å$^{-1}, E)$ of PC, measured at T = 300 K, using Eq. (1). The solid black line is $S(q, E)$, the solid blue line is the fit. The dashed lines are the fit components from three Lorentzians with Γ values indicated. Fit residuals, normalized to uncertainty in the data points, are shown in the upper part of the figure. Error bars throughout the text represent uncertainty at one standard deviation.

B. Elastic incoherent neutron scattering —Experimental

Elastic incoherent neutron scattering (EINS) measurements were performed at the NIST Center for Neutron Research on the High Flux Backscattering (HFBS) spectrometer[41] with an incident neutron wavelength of 6.271 Å, a 0.85 μeV full width at half-maximum energy resolution, and a momentum transfer (q) range of (0.25–1.35) Å^{-1}. The spectrometer was operated in the fixed-window mode where the elastic scattering intensity is recorded as a function of q while the sample was cooled at 1 K/min from 345 K to 4 K. The inelastic scattering was binned into 12 discrete q values, and the scattering intensity was integrated over the instrument resolution

$$I(q, \gamma_R) = \int_{-\gamma_R}^{\gamma_R} S(q, E) dE. \tag{7}$$

Intensity vs q data are shown in Fig. 2 for the temperatures indicated. Such data are typically analyzed assuming a harmonic oscillator model, i.e., assuming $S(q) \propto \exp(-3q^2\langle u^2\rangle)$, where $\langle u^2\rangle$ is a mean-squared displacement. The log(I) vs q^2 plots deviate significantly from linearity at low q but are approximately linear for higher q values. The common practice is to ignore the low q data and fit only the high q data with the harmonic oscillator model. Here, we use the more complete model in Eq. (1) for $S(q, E)$. The integration required by combining Eqs. (1) and (7) is trivial, as the Lorentzian terms are simply replaced by $2\pi^{-1}\arctan(\gamma_R/\Gamma_i)$.

The fixed window mode provides data at a single time point, $t_R = \hbar/\gamma_R \approx 2$ ns. On this time scale, terms containing Γ_v and Γ_h are not important, and only variations in Φ, Γ_D, σ_v, and σ_h impact the data fits. Fitting is performed by constraining Γ_D and σ_h to values obtained from fits to the DCS data and allowing σ_v and Φ to vary. The HFBS data and fits using Eqs. (1) and (7) are shown in Fig. 2. We obtain values for σ_v that are ≈50% larger than those obtained at 1 ps for the same temperatures. Alternatively, constraining Γ_D, σ_h, and σ_v leads to slightly degraded fits but similar Φ values.

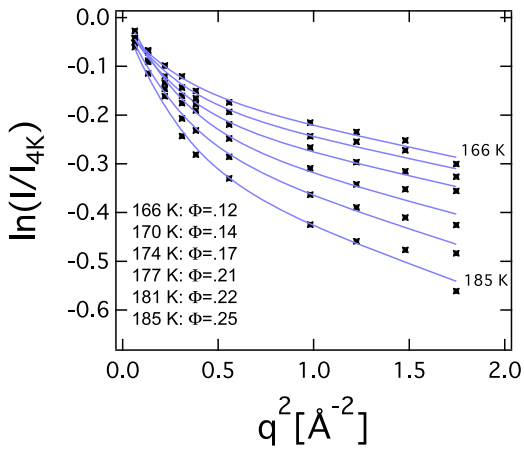

FIG. 2. Elastic scattering intensity as a function of q^2, T = 168, 175, 183, and 190 K, referenced against scattering acquired at 4 K. Solid lines are fits using Eqs. (1) and (7).

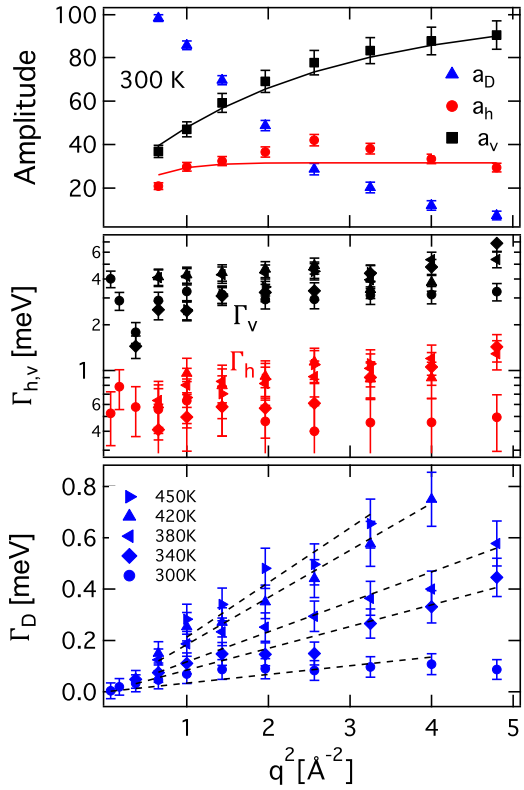

FIG. 3. Top panel: Amplitudes of Lorentzian components from fits of Eq. (1) to QENS data at 300 K. Solid lines are fits to Eq. (2). Middle panel: Dispersion relations for Γ_v (black symbols) and Γ_h (red symbols). Temperatures are indicated by symbol shape as shown in the bottom panel. Bottom panel: Dispersion relation for Γ_D at temperatures indicated. Dashed lines in the bottom panel are fits to the data.

C. Model veracity

The validity of our model is supported by its ability to simultaneously account for the full q-range of QENS and EINS data, and by the fact that fit values and trends for microscopic variables conform well to expectations based on decades of simulation work and experimentation. For example, the top panel of Fig. 3 shows a low-q amplitude rise of the most narrow Lorentzian component (a_D) indicating that it is not a localized mode, and the dependence of its spectral width on q and temperature clearly identifies it as a diffusive process.

The two remaining modes, v and h are expected to be localized, and this is also clearly the case. The low-q drop in scattering intensity observed in the top panel of Fig. 3 for these modes supports this assignment.[32] Also, the insensitivity of Γ_h and Γ_v to temperature we see in the middle panel of Fig. 3 indicates a small activation energy, as expected for a highly local motion.[31,42]

The time scales we obtain for the various modes are also consistent with previous work. We[19] and others[30] have previously assigned the intermediate process at $\tau_h \approx 1$ ps to spatially heterogeneous dynamics in the form of collective molecular rearrangements. Also, the fastest process we detect, with $\tau_v = 0.2$ ps, is typically associated with rapid, localized collisions between neighboring molecules occurring homogeneously throughout the sample. This motion is usually described as over-damped vibrations, although we will hereafter add clarity to this rather generic assignment.

The parameters for lengthscales of motion (σ_i) that we obtain by fitting the q-dependencies of the scattering amplitude parameters, a_i also support our model assignments. We fit a_i ($i = v$, h) using Eq. (2), as shown in the top panel of Fig. 3. From the fits, we obtain $\tilde{\sigma}_h = 0.2$ and $\tilde{\sigma}_v = 0.08$, where $\tilde{\sigma} = \sigma / r_H$, and $r_H = 2.6$ Å is the high-temperature hydrodynamic radius of PC.[43] These values correspond well to the relative average excursions for Lennard-Jones particles undergoing MB and IS and transitions, respectively.[15]

At first blush, it is perhaps surprising that we obtain such good agreement with $\tilde{\sigma}_v$ and $\tilde{\sigma}_h$ obtained from simulations of a highly simplified model system.[15] On the other hand, our view is that these motions are made possible by nearness of energetically similar packing configurations in the phase space. In other words, this is a packing-related problem, and so the absolute lengthscale should be determined primarily by molecular size and shape. In this case, we have normalized the lengthscale to the hydrodynamic radius of the molecule—which is a spherically averaged quantity, so, effectively the radius the molecule would take if it was spherical. Thus, the excellent correspondence to motion lengthscales obtained from spherical model systems is perhaps not so surprising.

Having some confidence that the model reasonably describes the dynamics of PC, we next explore the model parameters for the purpose of gaining a more clear understanding of microscopic dynamics in liquids.

D. Exploration of model fit parameters

Figure 4 shows $F(q, t)$, transformed to the time domain from $S(q, E)$ for PC at 300 K (see the supplementary material for transform details). The solid lines are fits to the transformed data using Eq. (3). The inset highlights the data and fits at small q, which are difficult to see in the main figure. It is clear that the overall relaxation is non-Gaussian, since a Gaussian

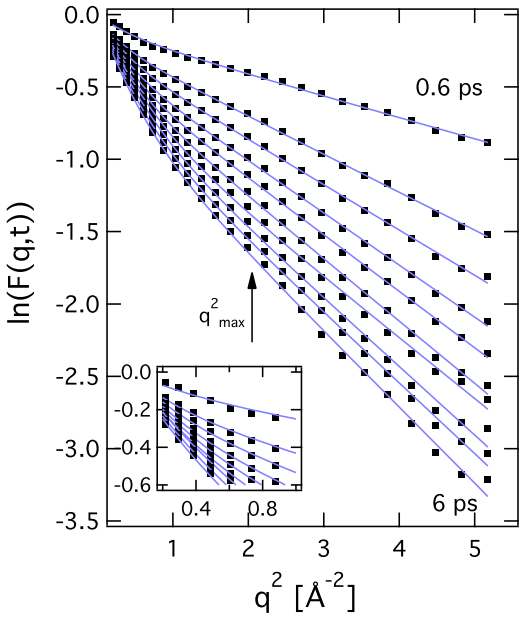

FIG. 4. $F(q, t)$ for PC at 300 K and times ranging from 0.6 ps to 6 ps in increments of 0.6 ps. Solid lines are fits to Eq. (3). Inset shows expanded low q region. The uncertainties in the data are approximately the size of the symbols.

response would result in a straight line on this plot. The two asymptotically linear regimes in the data confirm the existence of two distinct localized modes, as included in our model. In the time-domain fits, the low-q and high-q asymptotic slopes determine the values of σ_h and σ_v, respectively.

The format of Fig. 4 allows us to readily glean information about the nature of the v and h modes by considering the q-range of their influence. For reference, we indicate q^2_{max}, where $q_{max} = 1.45$ Å^{-1} is the maximum in the static structure factor for PC (see the supplementary material). The high-q linear regime, dominated by the v mode, spans regions on both sides of q_{max}, and so somehow appears to be pertinent to both intramolecular and intermolecular motions. By contrast, the low-q h mode appears to have only an intermolecular nature, as expected. The time-dependence of σ_i values provides further insight into the nature of these motions.

Figure 5 shows fit values $\tilde{\sigma}_v$ and $\tilde{\sigma}_h$ as a function of time for data obtained at temperatures ranging from 250 K to 380 K. The top panel displays $\tilde{\sigma}_h$ values, having amplitudes that conform with expectations for MB transitions,[15] as we have already mentioned. Additionally, the non-monotonic behavior is consistent with observations of de Souza and Wales,[44] who found evidence for successful and unsuccessful MB transition attempts. In agreement with that work, we have observed nonmonotonic behavior of σ_h in simulation and shown that it arises from molecular hopping associated with collective rearrangements[20] where a small number of molecules make large excursions in just a few steps, and some of them subsequently return to their origin.

The maxima in σ_h indicate the lifetime of the shortest-lived unsuccessful attempts at MB transitions. We note that these maxima occur at ≈1.2 ps, independent of temperature. This suggests that τ_h (also ≈1 ps and temperature independent) is a barrier crossing time for MB transitions.

The behavior of $\tilde{\sigma}_v$ suggests that it is related to IS transitions. The overall magnitude of the asymptotic values[15]

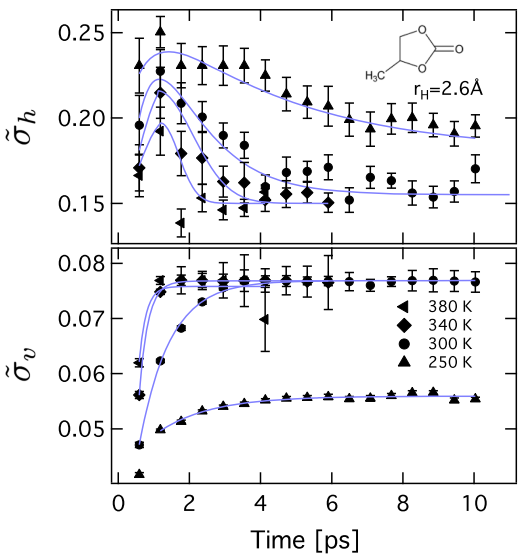

FIG. 5. Time dependence of $\tilde{\sigma}_v$ and $\tilde{\sigma}_h$ parameters derived from fits of Eq. (3) to $F(q, t)$ data in the range (250–380) K. The solid lines are fits to the data for the 250 K and 300 K and guides to the eye for the higher temperatures. Error bars indicate uncertainties in parameters at one standard deviation.

and the drop in these values beginning somewhat above the mode-coupling critical temperature[45] are consistent with that reported for IS transitions. Also, the rapid rise to a plateau suggests[46] the exploration of a bounded phase space, such as a series of IS transitions within a single MB. We suspect that individual IS transitions are too fast to be detected in the time-domain data (i.e., <0.5 ps). Several points of evidence support this conclusion. One is that we observe no reversing of IS, which are known to occur.[15] Another is that barriers for IS transitions are significantly smaller than those of MB transitions,[46] which we will see below occur on the order of 1 ps at high temperature. Finally, the characteristic time we obtain from the frequency domain for the v dynamic mode is 0.2 ps. We would expect that, analogous to the observations for the h mode, τ_v would be characteristic of barrier crossing events for individual IS transitions.

If this is correct and τ_v corresponds to barrier crossing for individual IS transitions, then the relatively slower rise in σ_v can be understood as a series of IS transitions that lead to exploration of an MB. This in turn would explain the precise correspondence we observe between the rise times in σ_v and the fall times after the maximum in σ_h and suggest that MB transition reversals would continue to occur as a system explores the new MB through IS transitions. The fact that we see evidence of reversing MB transitions over the entire timespan required for the exploration of the new MB attests to a relatively small configurational entropy for a MB. The time scale for the exploration of the MB, which we will call τ_{MX}, is ≈0.15 τ_α over the range that we can measure it.

Finally, we recall from Fig. 4 that the v mode appears to display some intermolecular character in addition to intramolecular property. IS transitions are expected to be somewhat cooperative, but we cannot separate effects of IS transitions from damped vibrations of individual molecules in the $\tilde{\sigma}_v$ response. We expect that the overdamped non-cooperative vibration contribution would reach a plateau value after only a few collisions (<100 fs), whereas the exploration of a MB through successive IS transitions could lead to σ_v values that increase over several ps as observed. We suggest that the velocity autocorrelation function would be a better response from which these effects can be separated.

We next explore the characteristic time for occurrence of MB transitions (τ_{TL}), which is contained in $\Phi(t)$. We will see that τ_{TL} is strongly temperature dependent and distinct from the temperature-independent barrier crossing time of individual MB transitions, τ_h. Of course, τ_{TL} could be as small as τ_h if saddle points for barrier crossing were somehow found instantaneously, but, since the MB is generally explored somewhat before the saddle point is found, $\tau_{TL} > \tau_h$ in general. Discovery of the saddle point through the exploration of an MB will be the rate-limiting step for MB transitions, so we may reasonably expect τ_{TL} to display a similar temperature dependence as τ_{MX}.

Figure 6 shows the time dependence of $(1 - \Phi(t))$ for a range of temperatures. At the lowest temperatures shown, no new molecules participate in MB transitions on the time scale of the QENS experiment and $\Phi(t) \approx \Phi_0$. This means that LC regions propagate very slowly or are ineffective at producing non-reversing MB transitions at these temperatures.

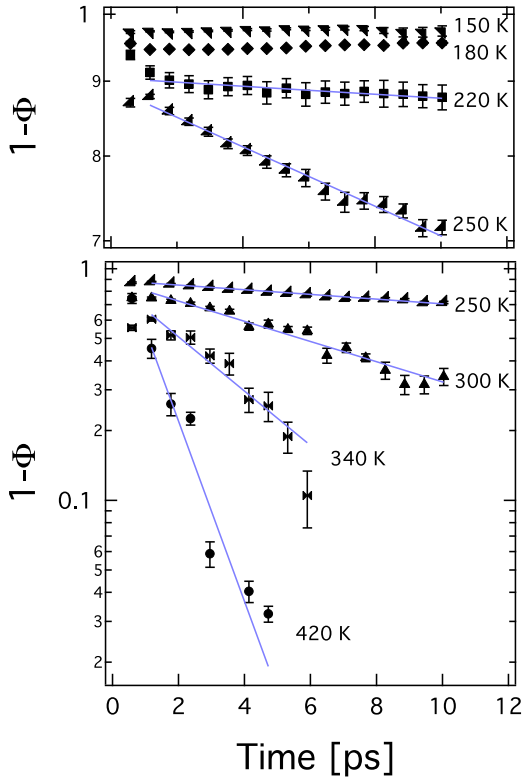

FIG. 6. Time dependence of Φ derived from fits of Eq. (3) to $F(q, t)$ for temperatures indicated. Dashed lines are exponential fits to the data.

By contrast, we directly observe an exponential decrease in $(1 - \Phi(t))$ at $T \geq 220$ K for $t \geq 1$ ps.

The τ_{TL} values obtained from QENS data at $T \geq 220$ K are plotted as solid circles in Fig. 7. At these high temperatures,

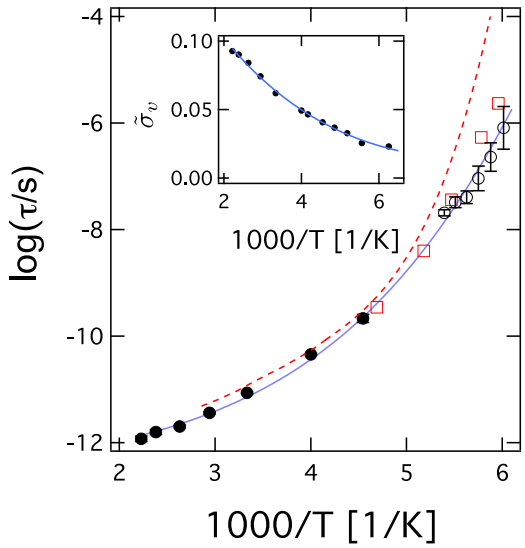

FIG. 7. PC relaxation times: (Black circles) τ_{TL} calculated from time dependence of Φ shown in Fig. 6. Error bars drawn are slightly smaller than the size of the symbols. (Solid blue line) Fit to τ_{TL} data using Eq. (8), with $\delta = 490 \pm 10$ J/mol and $\tau_0 = 0.32 \pm 0.03$ ps. (Black open circles) τ_{TL} calculated from fits of Eq. (9) to HFBS data. (Open squares) β_{JG} relaxation times from dielectric spectroscopy[47] and (dashed line) α relaxation times from dielectric spectroscopy[47] and light scattering.[48] The dielectric α and β data were reported as peak frequencies and were shifted together so that the dielectric α data coincide with α relaxation times from light scattering. Inset: $\tilde{\sigma}_{TC}$ values used as input to Eq. (8). The solid line in the inset is a polynomial fit.

$\tau_{TL} \approx 4\,\tau_{MX} \approx 0.6\,\tau_\alpha$. Values of τ_α are obtained from dielectric relaxation[47] and light scattering[48] and are represented by a dashed line in Fig. 7.

The relationship between τ_{TL} and τ_α at high temperatures suggests that MB transitions play an important role in α relaxation, as previously suggested.[22] While QENS τ_{TL} data seem to match up precisely with the $\tau_{\beta,JG}$ data, they are also not so different from the τ_α data, making it difficult to determine definitively which process it most closely corresponds to. Below we resolve this question through the use of a simple model for MB transitions and through the analysis of EINS data.

The Hall-Wolynes (HW) ansatz[49] seems to be appropriate for estimating τ_{TL} on time scales longer than we can directly measure with QENS. In fact, this model is perhaps even more fit for describing MB exploration and local barrier-crossings than the many-particle process implicated in α relaxation for which it was originally formulated. HW showed that, assuming potential wells can be approximated as parabolic near the bottom, and the barrier height between wells is proportional to the distance between their minima (r_0) in the configuration space, $log(k) \propto (r_0^2/\langle r^2 \rangle)$, where k is a transition rate and $\langle r^2 \rangle$ is a mean squared particle displacement within the well. Here, we use $\tilde{\sigma}_v$ to represent normalized displacements within the MB well (assuming $r_H \propto r_0$). We also allow for the fact that $\partial\tilde{\sigma}_v/\partial T \neq const.$ and so reformulate the HW relationship as

$$\tau_{TL} = \tau_0 \exp\left[\frac{\delta}{\tilde{\sigma}_v kT}\right]. \tag{8}$$

Figure 7 shows τ_{TL} values obtained from the data of Fig. 6, and a fit to those values using Eq. (8). The HW fit to τ_{TL} extrapolates precisely into the β_{JG} relaxation times, rather than the α relaxation times. Although suggestive, this is only an extrapolation, and we seek further evidence to determine which relaxation process the MB transitions should be associated with. That evidence is obtained from the EINS data.

As described in Section III B, we obtain $\Phi(t = 2$ ns) by fitting the EINS data to Eq. (1). Unlike the high-temperature QENS data, where we have many data points in the decay of $(1\text{-}\Phi(t))$, we have only two data points at low temperatures, Φ_0 from QENS and $\Phi(2$ ns) from EINS.

Having only two data points, we must assume a relaxation function. Our present purpose is to evaluate whether τ_{TL} corresponds to $\tau_{\beta JG}$ as indicated by fits of high temperature τ_{TL} to HW. Thus, we assume a Cole-Cole relaxation model for $\Phi(t)$ at low temperature, as is observed for β_{JG} relaxation. We then solve the following equation for τ_{TL}:

$$\frac{\Phi(t_R) - \Phi_0}{1 - \Phi_0} = \int_0^{\gamma_R} C(\omega, \tau_{TL})d\omega \Big/ \int_0^{\infty} C(\omega, \tau_{TL})d\omega, \tag{9}$$

where $C(\omega, \tau)$ is the imaginary component of the Cole-Cole distribution

$$C(\omega, \tau_{CC}) = -\mathrm{Im}\left[\frac{1}{1 + (i\omega\tau_{CC})^{1-\alpha_{CC}}}\right] \tag{10}$$

and where we have parameterized α_{CC} for PC as $\alpha_{CC} = -1.697 + 382/T$ by fitting the Cole-Cole dielectric β_{JG} data in Fig. 2 of Ngai *et al.*[47] with Eq. (10). Since τ_{CC} in Eq. (10) is the peak time of the relaxation distribution, the values of τ_{TL} that we retrieve from Eq. (9) can be directly compared to the

distribution peak values from the dielectric data. We calculate τ_{TL} values from EINS over a temperature range limited above by an instrument time window (the point at which $\tau_{TL} \leq 0.1\, t_R$) and below by T_g, since our PC sample was quenched relatively quickly.

Figure 7 includes τ_{TL} values from EINS and peak times for the β_{JG} relaxation time distribution from dielectric spectroscopy.[47] It is clear that these two measures correspond very well, and we thus confirm that individual MB transitions are indistinguishable from β_{JG} relaxation events based on their characteristic relaxation time, with the proviso that we have assumed (not directly measured) a Cole-Cole relaxation function for $\Phi(t)$ from EINS. As we review below, shared characteristics between β_{JG} and MB transitions, in addition to our finding of their identical time scales, strongly indicate that these are one and the same.

IV. DISCUSSION

A. Johari-Goldstein relaxation

The Johari-Goldstein relaxation[21] is an apparently universal phenomenon of non-crystalline systems,[29,47] but its precise nature has remained unresolved for almost 50 years. In recent decades, it has been proposed that β_{JG} relaxation should be associated with IS transitions[22] or exploration of MBs.[15] We have shown that, while both of these processes are too fast to be β_{JG}, transitions between MBs occur on a time scale identical to that of β_{JG} relaxation.

Our association between β_{JG} relaxation and MB transitions is supported by a significant body of evidence from the published literature. Included are the asymmetric double well behavior of β_{JG} relaxation,[27] the multi-step nature of both β_{JG}[26,28] and MB transitions,[15,16,46] the correspondence between rotational jump angles for β_{JG}[25,26,50] and jump distances for MB transitions,[15] and the fact that all molecules appear to participate in β_{JG}[26] relaxation and MB transitions,[15] although not all at once.

This association is also supported by the temperature dependence of the relaxation time distribution for the β_{JG} process. PC dielectric measurements of Ngai *et al.*[47] show that β_{JG} relaxation is highly non-exponential at low temperatures, but that the distribution of relaxation times narrows with increasing temperature, becoming exponential at approximately 225 K. Consistent with this, we observe an exponential behavior of the MB relaxation function $(1 - \Phi(t))$, at T ≥ 250 K with QENS.

One point of apparent discrepancy between β_{JG} and MB transition behavior involves the temperature dependence of their amplitudes. The strength of the latter is determined by Φ_0 and drops monotonically with reduced temperature, as shown here and in Ref. 19 whereas it has been reported that the β_{JG} relaxation strength drops with temperature only down to T_g, where it plateaus.[26] While it does appear that the ratio of the α and β_{JG} relaxation strengths reaches a plateau near T_g for some rigid glassformers,[51] this is not true for the absolute strength of the β_{JG} relaxation, which clearly continues to drop with reduced temperature even below T_g.[47,51–53] Thus, in this respect also, MB transitions behave as β_{JG} relaxations.

Connecting β_{JG} relaxation with MB transitions sheds light on the former as the latter have been characterized from a configuration space[46,54] and real-space[15,46,55,56] perspective. Of particular note is the work of Middleton and Wales[46] who characterized rearrangements associated with MB transitions ranging in energy and complexity, with some being similar to vacancy creation in crystalline solids.

B. Connection to other heterogeneous models of S(q, E)

Vispa *et al.*[31] have recently published the analysis of QENS on glycerol using a heterogeneous dynamics model that has some similarities to the model we propose. This report agrees with their work in several respects. Both reports find three distinct modes of motion in the respective liquids. One of these is diffusive, and the other two are localized. Further, both find that the time scales of the local modes are insensitive to temperature and approximately 200 fs and 1.2 ps. However, the reports differ in one important respect. Contrary to our report, Vispa *et al.* found the longer lengthscale motion to occur on the faster time scale. While we cannot say for sure why this would be, we can speculate.

One potential reason for the disagreement in assignment of local modes is a difference in the formulation of the models. Both include terms for vibration and hopping. However, the Vispa model assumes that some molecules only hop and others only vibrate. It seems to us that all molecules should undergo vibrations, and in fact the hopping process will be facilitated by intramolecular vibrations. Another important difference in the analysis of the QENS data is that Vispa *et al.* used a q-range limited to that below q_{max}, from 0.6 Å^{-1} to 1.3 Å^{-1} in order to avoid effects of coherent scattering. However, as we point out in our discussion of Fig. 4, much of the influence of the faster mode is observed at larger q values.

In addition to the evidence cited throughout the paper for our assignments of the v and h motions to fast and slow modes, respectively, we find additional indications that these assignments are correct. One is that our assignment agrees with results from a glassforming salt from Russina *et al.*,[30] who found a dynamic mode at ≈1 ps of extended spatial character that they identified with collective hopping motion and a faster mode associated with vibrations. Another is that, from simulation data on glycerol, we have found the collective mode to have a characteristic time of ≈1 ps.[20] Finally, circumstantial evidence is found in the top panel of Fig. 3. We find a slight excess in the fit amplitudes for a_h near q_{max}. It happens that the ratio of coherent to incoherent scattering from H^1 is also ≈5%, which roughly accounts for the excess observed in a_h. It thus appears that essentially all of the coherent scattering is manifested in this mode, identifying it with collective motion.

C. Connection to theoretical models of glass formation

In addition to providing qualitative insights into the dynamics of liquids, we show that, with appropriate modeling of $S(q, t)$, one can obtain values for microscopic variables that are used directly in theoretical models of liquids and glasses.

Microscopic theories are often tested indirectly by their ability to predict macroscopic phenomena, without being able to directly measure microscopic variables. For example, the facilitation theory has been used to reproduce fragility trends[36] or heat capacity data[57] without direct experimental access to confirm values of central controlling parameters c (the concentration of excitations) or τ_p (same as τ_{TL}). Here we have measured both of these quantities directly, making it possible to more critically evaluate the assumptions of that model. This will be the subject of future work.

Additionally, neutron methods under development[58] could be used to fully characterize the excitations on time scales from ps to μs and lengthscales from Angstroms to 10s of nanometers. Scattering data from such experiments, analyzed with the expression for S(q, E) found in Eq. (1), may allow us to develop a comprehensive picture of cooperative rearrangements, and provide direct constraints on the microscopic variables of models that focus on these motions in liquids and glasses.[59,60]

D. Dynamic heterogeneity?

Throughout this paper we have assumed that the observed motion on two distinct lengthscales is due to heterogeneous dynamics. This assumption is not without precedent, as we[19] and others[30,31] have previously presented evidence from neutron scattering for dynamically heterogeneous motion. Furthermore, there is overwhelming evidence for heterogeneous, collective dynamics from simulation.[15,24,55]

In spite of significant circumstantial evidence to the contrary, it is possible in principle that the distinct lengthscales of dynamics observed here arise from homogeneous dynamics. Thus, we briefly review the evidence for the heterogeneous dynamics case. Strong evidence can be found for short time DH in the time and temperature dependence of the scattering. Quite apart from the particular values of fit parameters, there are several trends in the scattering data that must be accounted for and are not compatible with homogeneous dynamics.

It is clear from the data in Fig. 4 that more than one lengthscale of motion contribute significantly to $F(q, t)$. A Gaussian q-dependence indicating a single characteristic lengthscale for motion would be represented by a straight line in this figure. By contrast, the data are apparently bi-linear and are fit very well with a simple two-Gaussian model. In a homogeneous model, distinct lengthscales can be explained only through anisotropic or intramolecular motion. Methyl rotor motion is the only possible intramolecular motion for PC; however, the characteristic lengthscale and time scale for the methyl rotor motion invalidate it as a candidate for either the v or h mode (see the supplementary material).

Anisotropic motion also appears not to be responsible for the two lengthscales of motion we see. Figure 8 shows the temperature dependence of $\tilde{\sigma}_h$ and $\tilde{\sigma}_v$ values obtained at 1 ps. The $\tilde{\sigma}_h$ values do not vary by more than 50% over the temperature range explored (60 K–450 K), whereas the $\tilde{\sigma}_v$ values change by almost a factor of 20 over this same range. The very different temperature dependencies of these two lengthscales could result from anisotropic motion only in the presence of significant temperature-dependent ordering in the liquid, for which there is no evidence. In the absence of such ordering, the ratio of lengthscales would be a function of the molecular geometry and temperature-independent.

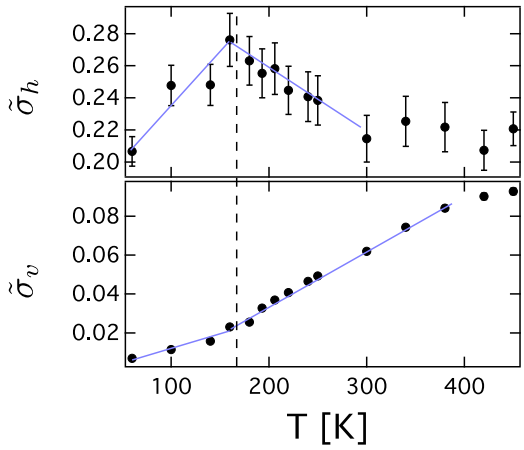

FIG. 8. $\tilde{\sigma}_v$ and $\tilde{\sigma}_h$ measured at 1 ps as a function of temperature. The solid lines are guides to the eye. The vertical dashed line marks T_g = 156 K for PC.

As with the temperature dependence of the ratio $\tilde{\sigma}_v/\tilde{\sigma}_h$, we know of no explanation based in homogeneous dynamics for the non-monotonic time-dependence of $\tilde{\sigma}_h$, or the fact that the intensity of the h mode increases with time. We thus conclude that the scattering signatures are indeed due to collective dynamics that are spatially and temporally heterogeneous.

V. CONCLUSIONS

We have modeled $S(q, E)$ with a scattering law that explicitly includes heterogeneous dynamics. Applying this model to quasielastic and elastic incoherent neutron scattering data of propylene carbonate, we identified motion that corresponds to the exploration of metabasins (MBs) through inherent state (IS) transitions and to MB transitions on a potential energy landscape (PEL). Having a direct approach to measure these dynamic features in real systems will provide important constraints to microscopic theories and will provide access to experimental regimes not accessible to simulation.

In spite of nearly 50 years of theoretical and simulation work on PELs, this is the first time to our knowledge that these classes of transitions have been identified in experimental data. Further, we were able to show directly for the first time that the characteristic time for MB transitions is identical to that of the Johari-Goldstein (β_{JG}) relaxation. We also believe that this is the first time β_{JG} relaxation has been identified from neutron scattering data, although Sperl previously proposed a Cole-Cole form for susceptibilities that accounted for dynamics observed over a similar lengthscale and time scale in optical Kerr effect data.[61] We note also that, very shortly after the first posting of a portion of this work,[62] Gupta *et al.*[63] also showed that β_{JG} relaxation could be obtained from EINS.

SUPPLEMENTARY MATERIAL

See supplementary material for detailed discussion of methyl rotor dynamics in PC and its relationship to our data analysis. It also includes details of data acquisition and pre-analysis data workup.

ACKNOWLEDGMENTS

The use of the HFBS spectrometer in this work is supported in part by the National Science Foundation under Grant No. DMR-1508249.

[1] K. Schmidt-Rohr and H. W. Spiess, Phys. Rev. Lett. **66**, 3020 (1991).
[2] M. T. Cicerone, F. R. Blackburn, and M. D. Ediger, Macromolecules **28**, 8224 (1995).
[3] M. T. Cicerone and M. D. Ediger, J. Chem. Phys. **103**, 5684 (1995).
[4] R. Böhmer, G. Hinze, G. Diezemann, B. Geil, and H. Sillescu, Europhys. Lett. **36**, 55 (1996).
[5] U. Tracht, M. Wilhelm, A. Heuer, H. Feng, K. Schmidt-Rohr, and H. W. Spiess, Phys. Rev. Lett. **81**, 2727 (1998).
[6] S. A. Reinsberg, A. Heuer, B. Doliwa, H. Zimmermann, and H. W. Spiess, J. Non-Cryst. Solids **307**, 208 (2002).
[7] Y. Z. Chua, G. Schulz, E. Shoifet, H. Huth, R. Zorn, J. W. P. Scmelzer, and C. Schick, Colloid Polym. Sci. **292**, 1893 (2014).
[8] R. Casalini, D. Fragiadakis, and C. M. Roland, J. Chem. Phys. **142**, 064504 (2015).
[9] R. Böhmer, R. V. Chamberlin, G. Diezemann, B. Geil, A. Heuer, G. Hinze, S. C. Kuebler, R. Richert, B. Schiener, H. Sillescu, H. W. Spiess, U. Tracht, and M. Wilhelm, J. Non-Cryst. Solids **235**, 1 (1998).
[10] F. H. Stillinger and T. A. Weber, Phys. Rev. A **28**, 2408 (1983).
[11] H. Miyagawa, Y. Hiwatari, B. Bernu, and J. P. Hansen, J. Chem. Phys. **88**, 3879 (1988).
[12] M. Goldstein, J. Chem. Phys. **51**, 3728 (1969).
[13] P. G. Debenedetti and F. H. Stillinger, Nature **410**, 259 (2001).
[14] R. A. Denny, D. R. Reichman, and J.-P. Bouchaud, Phys. Rev. Lett. **90**, 025503 (2003).
[15] M. Vogel, B. Doliwa, A. Heuer, and S. C. Glotzer, J. Chem. Phys. **120**, 4404 (2004).
[16] B. Doliwa and A. Heuer, Phys. Rev. E **67**, 030501 (2003).
[17] F. W. Starr, J. F. Douglas, and S. Sastry, J. Chem. Phys. **138**, 12A541 (2013).
[18] P. Charbonneau, Y. Jin, G. Parisi, and F. Zamponi, Proc. Natl. Acad. Sci. U. S. A. **111**, 15025 (2014).
[19] M. T. Cicerone, Q. Zhong, and M. Tyagi, Phys. Rev. Lett. **113**, 117801 (2014).
[20] M. T. Cicerone, D. Averett, and J. J. de Pablo, J. Non-Cryst. Solids **407**, 118 (2015).
[21] G. P. Johari and M. Goldstein, J. Chem. Phys. **53**, 2372 (1970).
[22] F. H. Stillinger, Science **267**, 1935 (1995).
[23] D. Thirumalai and R. D. Mountain, Phys. Rev. E **47**, 479 (1993).
[24] F. H. Stillinger and T. A. Weber, Science **225**, 983 (1984).
[25] I. Chang, F. Fujara, B. Geil, G. Heuberger, T. Mangel, and H. Sillescu, J. Non-Cryst. Solids **172**, 248 (1994).
[26] M. Vogel and E. Rössler, J. Phys. Chem. B **104**, 4285 (2000).
[27] J. C. Dyre and N. B. Olsen, Phys. Rev. Lett. **91**, 155703 (2003).
[28] M. Vogel, C. Tschirwitz, G. Schneider, C. Koplin, P. Medick, and E. Rössler, J. Non-Cryst. Solids **307**, 326 (2002).
[29] H. B. Yu, W. H. Wang, H. Y. Bai, and K. Samwer, Natl. Sci. Rev. **1**, 429 (2014).
[30] M. Russina, F. Mezei, R. Lechner, S. Longeville, and B. Urban, Phys. Rev. Lett. **84**, 3630 (2000).
[31] A. Vispa, S. Busch, J. L. Tamarit, T. Unruh, F. Fernandez-Alonso, and L. C. Pardo, Phys. Chem. Chem. Phys. **18**, 3975 (2015).
[32] A. Rahman, K. S. Singwi, and A. Sjölander, Phys. Rev. **126**, 986 (1962).
[33] U. B. Sjolander, W. Gotze, and A. Sjolander, J. Phys. C: Solid State Phys. **17**, 5915 (1984).
[34] T. Kawasaki, T. Araki, and H. Tanaka, Phys. Rev. Lett. **99**, 215701 (2007).
[35] M. Leocmach and H. Tanaka, Nat. Commun. **3**, 974 (2012).
[36] J. P. Garrahan and D. Chandler, Proc. Natl. Acad. Sci. U. S. A. **100**, 9710 (2003).
[37] A. Ottochian and D. Leporini, J. Non-Cryst. Solids **357**, 298 (2011).
[38] Y. Jung, J. P. Garrahan, and D. Chandler, Phys. Rev. E **69**, 061205 (2004).
[39] F. Qi, G. Hinze, R. Böhmer, H. Sillescu, and H. Zimmermann, Chem. Phys. Lett. **328**, 257 (2000).
[40] J. R. D. Copley and J. C. Cook, Chem. Phys. **292**, 477 (2003).
[41] P. M. Gehring and D. A. Neumann, Physica B **241**, 64 (1997).
[42] F. Fernandez-Alonso, S. E. McLain, J. W. Taylor, F. J. Bermejo, I. Bustinduy, M. D. Ruiz-Martín, and J. F. C. Turner, J. Chem. Phys. **126**, 234509 (2007).
[43] F. Qi, K. U. Schug, S. Dupont, A. Doss, R. Bohmer, H. Sillescu, H. Kolshorn, and H. Zimmermann, J. Chem. Phys. **112**, 9455 (2000).
[44] V. K. de Souza and D. J. Wales, J. Chem. Phys. **129**, 164507 (2008).
[45] J. Hernández-Rojas and D. J. Wales, J. Non-Cryst. Solids **336**, 218 (2004).
[46] T. F. Middleton and D. J. Wales, Phys. Rev. B **64**, 024205 (2001).
[47] K. L. Ngai, P. Lunkenheimer, C. Leon, U. Schneider, R. Brand, and A. Loidl, J. Chem. Phys. **115**, 1405 (2001).
[48] W. M. Du, G. Li, H. Z. Cummins, M. Fuchs, J. Toulouse, and L. A. Knauss, Phys. Rev. E **49**, 2192 (1994).
[49] R. W. Hall and P. G. Wolynes, J. Chem. Phys. **86**, 2943 (1987).
[50] M. Saito, S. Kitao, Y. Kobayashi, M. Kurokuzu, Y. Yoda, and M. Seto, Phys. Rev. Lett. **109**, 115705 (2012).
[51] A. Kudlik, S. Benkhof, T. Blochowicz, C. Tschirwitz, and E. Rössler, J. Mol. Struct. **479**, 201 (1999).
[52] G. P. Johari, Ann. N. Y. Acad. Sci. **279**, 117 (1976).
[53] A. Kudlik, C. Tschirwitz, S. Benkhof, T. Blochowicz, and E. Rössler, Europhys. Lett. **40**, 649 (1997).
[54] B. Doliwa and A. Heuer, Phys. Rev. E **67**, 031506 (2003).
[55] A. S. Keys, L. O. Hedges, J. P. Garrahan, S. C. Glotzer, and D. Chandler, Phys. Rev. X **1**, 021013 (2011).
[56] S. S. Schoenholz, E. D. Cubuk, D. M. Sussman, E. Kaxiras, and A. J. Liu, Nat. Phys. **12**, 469 (2016).
[57] A. S. Keys, J. P. Garrahan, and D. Chandler, Proc. Natl. Acad. Sci. U. S. A. **110**, 4482 (2013).
[58] R. Gähler, R. Golub, and T. Keller, Physica B **180**, 899 (1992).
[59] G. Adam and J. H. Gibbs, J. Chem. Phys. **43**, 139 (1965).
[60] T. R. Kirkpatrick, D. Thirumalai, and P. G. Wolynes, Phys. Rev. A **40**, 1045 (1989).
[61] M. Sperl, Phys. Rev. E **74**, 011503 (2006).
[62] M. T. Cicerone and M. Tyagi, preprint arXiv:1607.07393 (2016).
[63] S. Gupta, J. K. H. Fischer, P. Lunkenheimer, A. Loidl, E. Novak, N. Jalarvo, and M. Ohl, preprint arXiv:1609.06822 (2016).